International Journal of Hybrid Information Technology
Vol.9, No.2 (2016), pp. 329-338
http://dx.doi.org/10.14257/ijhit.2016.9.2.29

A Novel Algorithm for Tracking and Forecasting Convective Cells Using Satellite Image Sequences

Jia Liu[1], Chuancai Liu[1], Chao Ma[1], Danyu Qin[2] and Furong Peng[1]

[1]*Nanjing University of Science and Technology, School of Computer Science and Engineering, 200 Xiaolingwei Street, Nanjing, China, 210094*
[2]*China Meteorological Administration, National Satellite Meteorological Center, 46 Zhongguancun South Street, Beijing, China, 100081*
sqzyliujia@163.com

Abstract

Accurate storm tracking and forecasting are essential parts of severe weather warning operations. The main problem of existing tracking and forecasting algorithms is unphysical split and merger of cloud clusters within the life cycle of Mesoscale Convective System (MCS). To address this issue, an automatic algorithm called TFCC (Tracking and Forecasting Convective Cells) is proposed for tracking and forecasting convective cells using infrared (IR) image sequences from geostationary meteorology satellite. In this paper, convective cells are utilized for tracking and forecasting instead of MCS because convective cells are stable portion in MCS. TFCC algorithm utilizes overlapping technique and uses a dynamic constraint technique based combinatorial optimization method. Moreover, displacement of the geometrical centroid is utilized to forecast the movement of convective cells. Case studies show that convective cells are tracked and forecasted efficiently in different phases of MCS lifecycle including genesis, maturity and dissipation using TFCC algorithm. Categorical statistics and contingency tables method applied to various case studies over China show that TFCC algorithm efficiently and accurately.

Keywords*: Mesoscale Convective System, convective cells, tracking, forecasting*

1. Introduction

Mesoscale Convective System (MCS), which is a convective phenomenon, plays a vital role in dominating the rainfall over China [1–3]. Convective cells are crucial element of MCS and associated with hazardous consequences, and generate a lot of rain during the monsoon period [4, 5]. Convective cells can be detected and tracked by radar or satellite. Radar has a limited coverage and no possibility to detect a developing convective cell [6]. The alternative source is satellite data. Compared with radar, satellite provides higher coverage.

A group of detecting and tracking techniques of MCS have been developed in the past decades [4–8]. Threshold methods [7, 8] depend on the brightness temperature (Tb) threshold, usually provide unreliable detection results. ETITAN (enhanced thunderstorm identification, tracking, and nowcasting) algorithm uses multi-threshold to identify convective cell, and proposes a dynamic constraint-based combinatorial optimization method to track storms [9, 10]. These techniques provide enhancements to the original TITAN (thunderstorm identification, tracking, and nowcasting) algorithm, however, sometimes they provide inaccurate identification, tracking, and forecasting results. FORTRACC [15] (forecast and tracking the evolution of cloud clusters) is an algorithm for tracking and forecasting radioactive and morphological characteristics of MCS using geostationary satellite image. A variational-data-assimilation tool was developed to track

ISSN: 1738-9968 IJHIT

and analyze convective cloud systems [4, 5], whereas, the technique is time-consuming. Source apportionment (SA) approach was presented to track and forecast MCS [16]. An algorithm named TOOCAN (tracking of organized convection algorithm through a 3-D segmentation) was designed to detect and track MCS based on an iterative process of 3-D segmentation using the infrared imagery from geostationary satellite over the tropics [17]. However, this method is required to handle real-time problem. A method for detecting and tracking rainfall clouds in non-Doppler radar images can be usefully exploited by radar operators to automatically detect, characterize, and follow the precipitation fields in real time [11]. However, the primary method for tracking remains the area-overlapping techniques [12–14].

MCS detecting, which is usually implemented by threshold methods [16], is the basis of tracking and forecasting of MCS. Detection methods proposed by various researchers use a Tb value to depict continuous areas of deep convective cloudiness [17]. Tb threshold below 241 K are usually utilized to detect convective areas [18]. The definition of genesis, maturity and dissipation is closely associated with the coldest cloud top area [19]. Another significant factor is the continuous selection of the pixels as mentioned in the definition of MCS [16, 18].

At the tracking and forecasting stage, unphysical splitting and merging of cloud clusters within the life cycle of the MCS remains a significant problem [17]. To address this issue, we present an automatic algorithm called TFCC for tracking and forecasting convective cells using geostationary satellite IR image sequences. In this paper, convective cells are utilized for tracking and forecasting instead of MCS because convective cells are stable portion in MCS. Moreover, some morphological operations [9, 20] have been proposed to improve the track ability of storms. Inspired by TITAN method, ETITAN method and FORTRACC algorithm, we utilize overlapping technique and dynamic constraint technique based combinatorial optimization method to track convective cells. Moreover, trajectory (displacement of the geometrical centroid) is utilized to forecast the movement of convective cells.

In this paper, Section 2 introduces the methods used for convective cells tracking and forecasting. Section 3 describes experiment data and three case studies, while Section 4 describes validation methods. Summary and conclusions are presented in a subsequent Section.

2. Methods

2.1 Mathematical Morphology Descriptions

In grayscale mathematical morphology, structuring element is used to probe or interact with a given image, drawing conclusions on how this shape fits or misses the shapes in the image [20]. Grayscale structuring elements are called "structuring functions". An image is denoted by f(x) and the structuring function is denoted by b(x), the grayscale dilation is given by

$$(f \oplus b)(x) = \sup_{y \in E}[f(y) + b(x-y)] \tag{1}$$

Where "sup" denotes the supremum of a function. Similarly, the grayscale erosion is given by

$$(f \ominus b)(x) = \inf_{y \in E}[f(y) - b(y-x)] \tag{2}$$

Where "inf" denotes infimum of a function. Opening is erosion followed by dilation, which is given by

$$f \circ b = (f \ominus b) \oplus b \tag{3}$$

Close operation is given by

$$f \bullet b = (f \oplus b)!\ \ b \tag{4}$$

H-maxima transform suppresses all maxima which below or equal to a given threshold in the intensity image [20]. Therefore, H-maxima transform which is applied to convective cells detection can avoid separation of the maxima points within the same cell. H-maxima transform is given by

$$HMAX_h(X) = R_f^{\delta}(X - h) \tag{5}$$

Where X denotes original image, h denotes threshold, R_f^{δ} denotes dilate reconstruction.

The regional extremum, which is computed by the pixel value of an original image minus H-maxima, is given by

$$RMAX_h(X) = X - R_f^{\delta}(X - h) \tag{6}$$

Extended maxima, which is defined as the regional minima of the H-maxima, is given by

$$EMAX_h(X) = RMAX[HMAX_h(X)] \tag{7}$$

This method extracts seed point of convective cells more efficiently and provides a good foundation for later convective cells tracking and forecasting. For more information about these terms, please refer to our previous work [21].

2.2 The Details of TFCC Algorithm

At the MCS detection stage, we proposed an algorithm named extended maxima transform based region growing (EMTRG) [21] to detect MCS. This algorithm uses region growing method to identify contiguous pixels. In this paper, some morphological operations have been suggested to improve the track ability of storms before tracking.

At the tracking stage, the main method for tracking remains the area-overlapping technique. This technique assume that a cloud at next time frame corresponds to that at last time frame, considering the previous constraints of size and temperature, there are common pixels in consecutive images [15]. The comparison of successive satellite images is carried out forward and backward in time [13, 14], so there are five types of possible situations: spontaneous generation, natural dissipation, continuity, split and merger (see Figure 1). Figure 1(a) shows the intersection of the surfaces area respectively occupied by a convective cell in an image and the following one, which is continuity mentioned above. Split and merger are more complicated situation as illustrated in Figure1 (b) and Figure 1 (c).

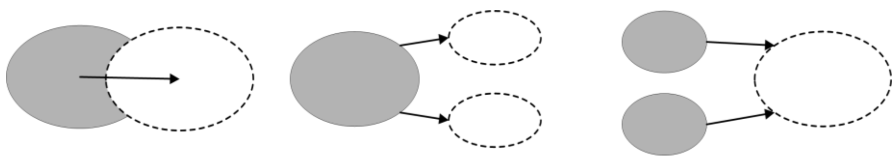

(a) (b) (c)

Figure 1. Three Types of Possible Tracking Situations. The Gray Ellipse Represents MCS in The first Time Step while White Dotted Ellipse Represents the Next Time Step. (a) Continuity, (b) Split, and (c) Merger

Unphysical splitting and merging of cloud clusters strongly limit the use of MCS tracking and forecasting results. The main problem of existing tracking algorithms is split and merger events [17]. To address this issue, we present an automatic algorithm called TFCC for tracking and forecasting convective cells using geostationary satellite IR image sequences. Inspired by TITAN and ETITAN method, TFCC algorithm adopts overlapping technique and then uses a dynamic constraint technique-based combinatorial optimization method [9]. Hungarian method [22, 23] is utilized to solve the combinatorial optimization problem similar to TITAN algorithm. At the forecasting stage, trajectory (displacement of the geometrical centroid) is utilized to forecast the movement of convective cells instead of using motion vector field of MCS in ETITAN algorithm. The procedure of TFCC algorithm is given below:

Algorithm 1 Tracking and Forecasting Convective Cells (TFCC)

Input: Successive satellite image data X
Initialization:
    Set Tb threshold T=241K.
    while Tb >T
        Tb $\leftarrow$ 0
    end while
Detection:
    Compute convective cells using EMTRG algorithm.
Tracking:
    Preprocessing using morphological operations according to Eq. (1)-(4).
    Overlapping technique and Hungarian method are utilized to tracking each convective cell.
Forecasting:
    Displacement of the geometrical centroid is used to forecast movement of convective cells.
Output: Results T

3. Satellite Data and Case Studies

3.1 Satellite Data

In this paper, IR data from FY-2F (fengyun-2F geostationary meteorological satellite) of China are used for the case study. A five-channel visible and infrared spin scan radiometer and a space environment monitor are main payloads of FY-2F (Table 1).

Table 1. FY-2F Satellite Imager Radiometric Channels

Channel	Wavelength (μm)	Spatial Resolution (km)	Used
IR1	10.3-11.3	5	√
IR2	11.5-12.5	5	√
IR3	6.3-7.6	5	√
IR4	3.5-4.0	5	
VIS	0.55-0.90	1&5	

IR image sequences with time intervals 6 minutes and spatial resolution 5 km in August 2014 have been selected for case study of convective cells tracking and forecasting. We tried experiment with multiple-channels and found that 10.3-11.3μm IR channel can get the best tracking and forecasting results. Therefore, data from FY-2F in the 10.3-11.3μm IR channel (*i.e.*, IR1) are used for case study in this paper.

3.2 Case Studies

Brightness temperature image reflects the Tb difference of clouds. Various approximate outlines of convective cells can be observed in brightness temperature image (red and yellow portion). Detection results compare with the red and yellow portion in brightness temperature image to verify the efficiency of EMTRG algorithm during MCS lifecycle. EMTRG algorithm proposed by us can distinguish adjacent region of convective cells efficiently, and provides a good foundation for later convective cells tracking and forecasting.

In this section, the efficiency of TFCC algorithm for convective cells tracking and forecasting is illustrated using IR image sequences. In China, rainstorms occur frequently in August. Therefore, 10.3-11.3 μm IR image sequences with 6 minutes time intervals and spatial resolution of 5 km in August 2014 are selected for case study. The following three case studies represent three complex scenes which contain different phases of MCS life cycle including genesis, maturity and dissipation. The first case study over South China will be discussed in more details.

Figure 2 shows tracking schemes over a selection of images for the convective situation which occurred over the region of South China at 1424 UTC August 27, 2014. Figure 2(a) is the original IR image and it contains several cloud clusters. Figure 2(b) represents the corresponding brightness temperature images of Figure 2(a), which indicate the different values of Tb for clouds. An approximate contour of all convective cells (see the red portions) can be seen in the brightness temperature images. Figure 2(c) depicts the corresponding result (colored contour and its interior) of convective cells detection using EMTRG [21] algorithm and tracking resulting using TFCC algorithm. We use the same color to identify the contour of matched convective cells in successive image. First of all, we can observe subjectively that EMTRG algorithm identifies MCS much as one would do from viewing the infrared images. The capability of detecting convection in its triggering stage is vital in a perspective of forecast applications [17]. EMTRG algorithm can detect different phases of MCS lifecycle including genesis, maturity and dissipation. Note that EMTRG algorithm identifies 30 convective cells for this period (Figure 2(c)). Convective cells are superimposed on the original image to make it clear, note that the contour of the cells is consistent with the approximate contour of convective cells shown in brightness temperature images. Figure 2(d) depicts the result (colored contour and its interior) of convective cells detection using EMTRG algorithm after 30 min. Note that each red arrow in Figure 2(c) directs to the center of mass of matched convective cell in Figure 2(d). The red box and the purple box in Figure 2(c) depict merge events processed by TFCC algorithm. Note that the two red arrows in the red box are direct to the same position where is the centroid of matched convective cell in the red box of Figure 2(d). The green color convective cell in red box in Figure 2(d) is the matched object of the green and purple convective cells in the red box in Figure 2(c) using TFCC algorithm. It is obvious that the red box in Figure 2(d) only one convective cell survives, which is merged from the last frame. Similar to the red box, the purple box in Figure 2(c) and Figure 2(d) demonstrate the same processing using TFCC algorithm. The area evolution of other convective cells are smooth because no split or merge events take place.

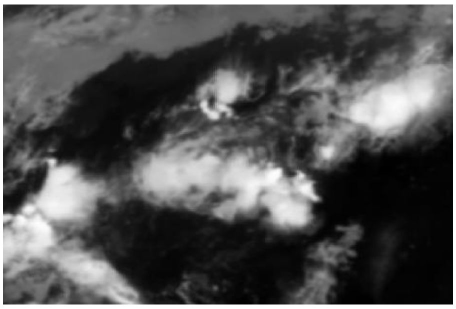

(a)

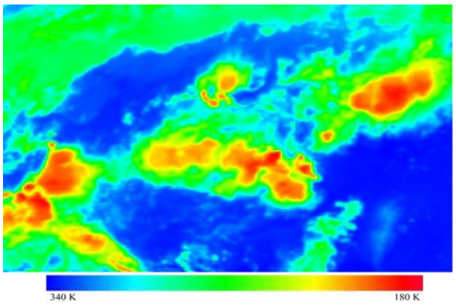

(b)

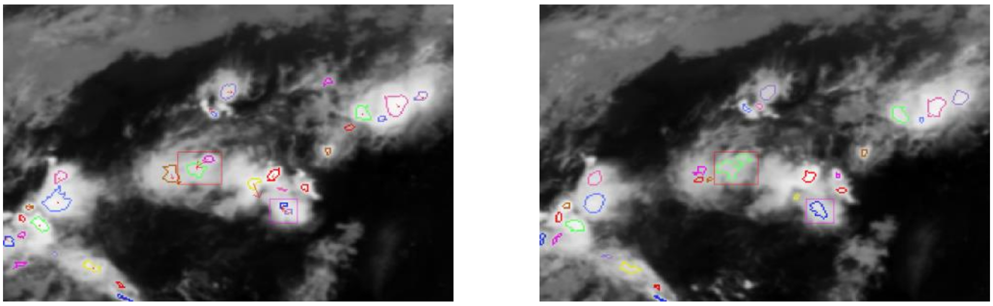

(c) (d)

Figure 2. 30 min Intervals Convective Cells Tracking which Occurred Over the Region of South China at 1424 UTC August 27, 2014. (a) The Original IR Image. (b) The Corresponding Brightness Temperature Image. (c) Results of 30 min Intervals Convective Cells Tracking. (d) Convective Cells Detection using EMTRG Algorithm with 30 min Intervals

Figure 3 shows the tracking results for the convective situation which occurred over the region of South China at 1524 UTC August 27, 2014. Note that EMTRG algorithm identifies MCS much as one would do from viewing the Tb images (Figure 3(b)). EMTRG algorithm identifies 27 convective cells for this period (see Figure 3(c)). Figure 3(c) illustrates tracking result of MCS by TFCC algorithm. Figure 3(d) depicts the result (colored contour and its interior) of convective cells detection after 60 min using EMTRG algorithm. Each red arrow in Figure 3(c) directs to the centroid of matched convective cell in Figure 3(d). This case study has several dissipation events occur, here we only demonstrate one. The red box in Figure 3(c) contains 4 convective cells, depicts dissipation events occurrence dealt with by TFCC algorithm. Note that there are not any arrows survive in the red box in Figure 3(c) because the 4 convective cells dissipation in the next time frame. We can observe that no convective cell survive in the red box in Figure 3(d) because the 4 convective cells in the red box in Figure 3(c) dissipation in this time frame.

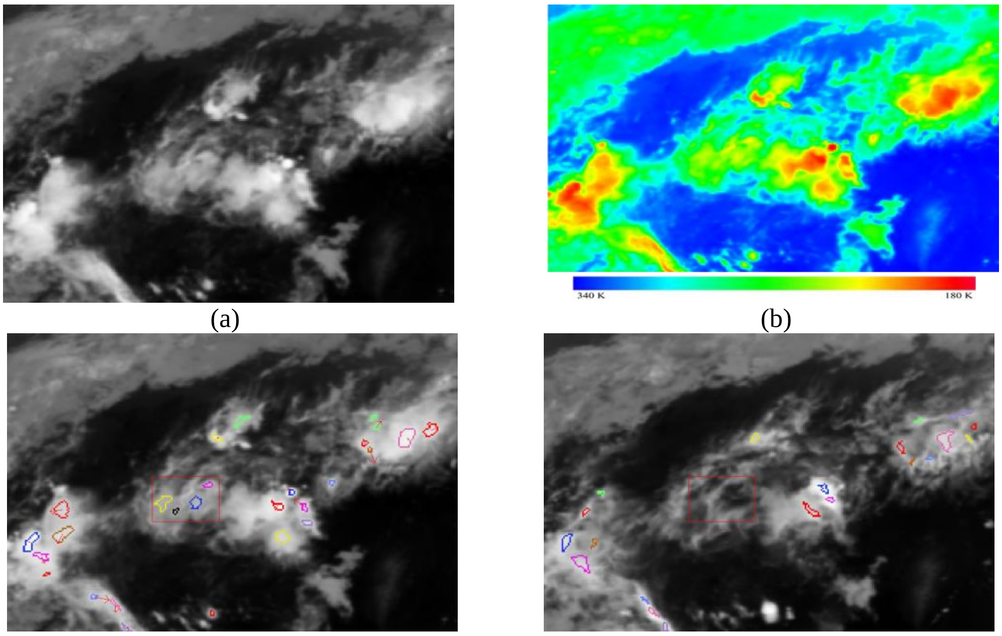

(a) (b)

(c) (d)

Figure 3: 60 min Intervals Convective Cells Tracking which Occurred Over the Region of South China at 1524 UTC August 27, 2014. (a) The Original IR

Image. (b) The Corresponding Brightness Temperature Image. (c) Results of 60 min Intervals Convective Cells Tracking. (d) Convective Cells Detection using EMTRG Algorithm with 60 min Intervals

Figure 4 shows tracking schemes over a selection of images for the convective situation which occurred over the region of East China at 1030 UTC August 28, 2014. This case study shows the most complex situation and contains the most convective cells. EMTRG algorithm identifies 61 convective cells for this period (Figure 4(c)). Convective cells are superimposed on the original image for clear to understand. Figure 4(d) depicts the result (colored contour and its interior) of convective cell detection using EMTRG algorithm after 90 min. This case study shows the EMTRG algorithm to detect small MCS efficiency, especially the right top of Figure 4(c). Over the tropical region, the detecting of small MCS is pivotal because large population of MCS has short lifetime duration [24].

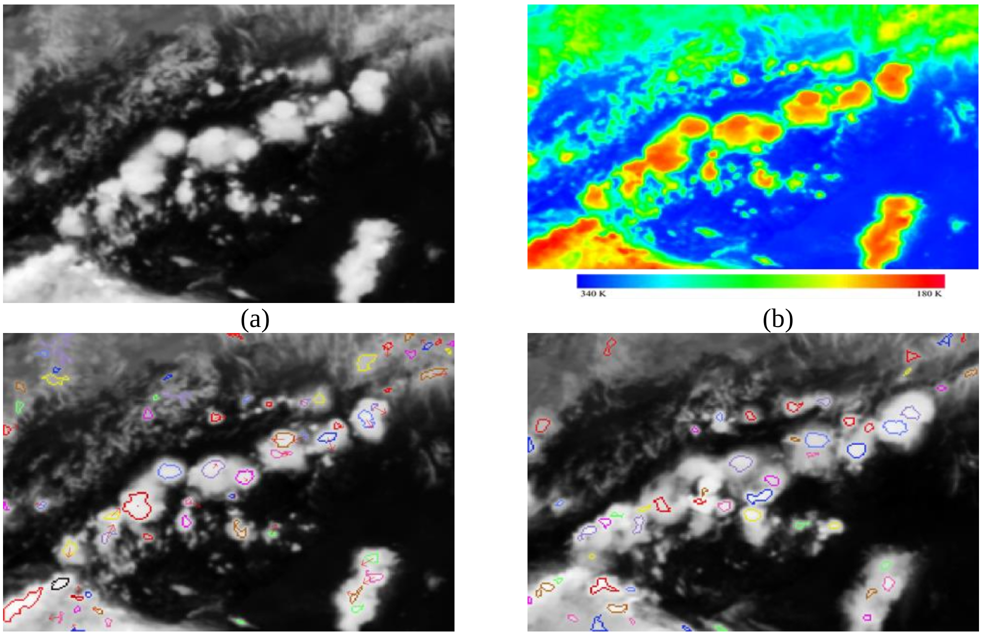

(a) (b) (c) (d)

Figure 4. 90 min Intervals Convective Cells Tracking which Occurred Over the Region of East China at 1030 UTC August 28, 2014. (a) The Original IR image. (b) The Corresponding Brightness Temperature Image. (c) Results of 90 min Intervals Convective Cells Tracking. (d) Convective Cells Detection using EMTRG Algorithm with 90 min Intervals

The analysis of these case studies illustrates the issues caused by merger and dissipation. It has also emphasized the capacity of TFCC algorithm to deal with these issues, for different tropical regions or organized convective situations in MCS lifecycle.

4. Validation Method

The subjectivity inherent in the tracking of MCS enhances the difficulty to evaluate and to validate a new tracking algorithm [17]. However, it is vital to evaluate its capacity to track MCS and then to have a measure of its efficiency. Several methods have been developed to evaluate tracking algorithm [9, 25–29]. Contingency tables method and Categorical statistics were utilized to evaluate our algorithm in this paper [28, 29].

4.1 Contingency Tables Method

To the best of our knowledge, MCS life cycles with frequent splits and mergers are difficult to validate. A contingency tables method was implemented to measure the TFCC algorithm skill. This validation process takes into consideration all of situations since many life cycles have merger and split events. The four combinations of forecasts and observations are defined as follows: (1) Correct negative: Tb of the forecasted and observed pixel is above 241 K. (2) False alarm: Tb of the forecasted pixel is below 241 K while the observed temperature is above 241 K. (3) Hit: Tb of the forecasted and observed pixel is below 241 K. (4) Miss: Tb of the forecasted pixel is above 241 K while the observed temperature of that pixel is below 241 K.

In contingency table method, various statistical indexes were calculate to describe particular aspects of forecast performance like accuracy (ACU), bias score (BIAS), probability of detection (POD), and false alarms rate (FAR) [28, 29]. ACU is the score of correctly forecasted pixels compared with the total number of pixels. The BIAS score measures the error between the number of pixels predicted as MCS (Tb <241 K) and the number of pixels observed as MCS (Tb < 241 K). POD denotes the observed pixels that have been correctly predicted. FAR denotes a pixel with Tb < 241K is predicted but it is not observed.

Table 2 indicates the statistical indexes for 30, 60, 90, and 120 min forecast. ACU shows larger values for 30 min forecast lead time, 89% of the pixels have been correctly predicted. This value is high because most of the values correspond to correct negative pixels (Tb<241 K). POD of 30 min forecast reaches approximately 0.88 and FAR is around 0.09. That is to say, while 88% of the observed pixels corresponding Tb<241 K were correctly forecasted, 9% of the forecasted pixels were not observed. For the 120 min forecast, ACU index is about 0.84 for the period, POD and FAR seem to be somewhat too far from the desired situation.

Table 2. POD, FAR, ACU, BIAS for 30 min, 60 min, 90 min and 120 min Forecast Lead Times for the Period 1-30 August 2014

Time	30 min	60 min	90 min	120min
POD	0.89	0.86	0.85	0.83
FAR	0.09	0.10	0.12	0.13
ACU	0.89	0.88	0.86	0.84
BIAS	0.88	0.86	0.85	0.82

4.2 Categorical Statistics

Figure 5 is an example of time evolution of the number of MCS pixels observed and predicted (Tb<241 K) for the entire image for 30 min, 60 min, 90 min, and 120 min forecast lead times for the period 10-16 August 2014. Note that the diurnal cycle is correctly forecast. The mean amount of observed pixels is slightly higher than the mean value of the predicted ones for the same period. With the forecast time grows, the error number of forecast pixels gradually increasing. Most error situation is obtained for 120 min forecast lead time (Figure 5(d)), where the larger underestimations are present. This reason for this is that the behavior of MCS is more complex with initiation, dissipation, merger, split, frequent regenerations, and spontaneous generation *etc*.

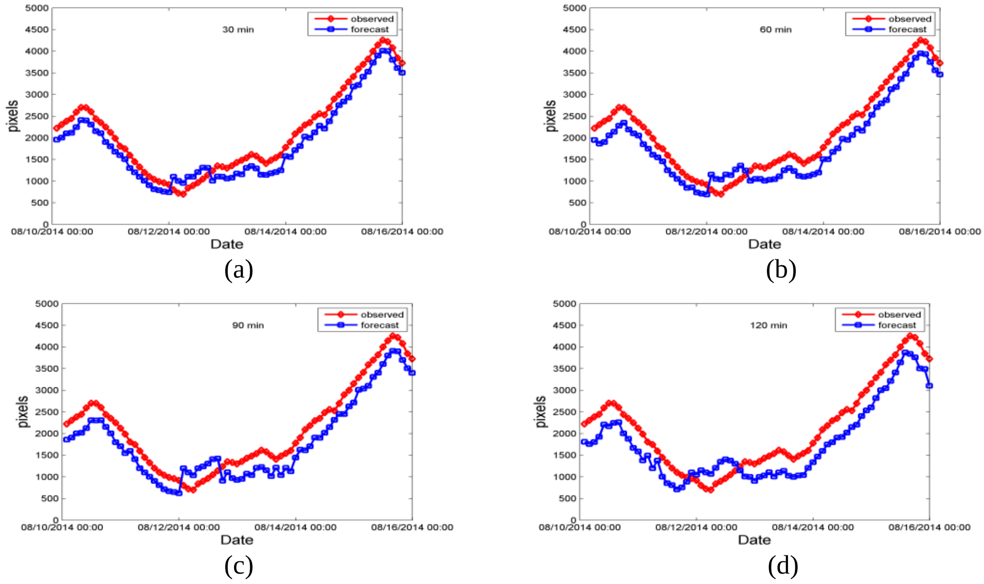

Figure 5: Number of Observed and Forecasted MCS Pixels per Image during the Period 10-15 August 2014. (a) 30 min Forecast. (b) 60 min Forecast. (c) 90 min Forecast Range. (d) 120 min Forecast

5. Summary and Conclusions

A novel algorithm named TFCC is developed in this paper for tracking and forecasting convective cells. Inspired by TITAN method, ETITAN method and FORTRACC algorithm, we utilize overlapping technique and dynamic constraint technique based combinatorial optimization method to track convective cells. Moreover, trajectory (displacement of the geometrical centroid) is utilized to forecast the movement of convective cells instead of using motion vector field of MCS in ETITAN algorithm. Convective cells are utilized for tracking and forecasting instead of MCS in our algorithm. Some morphological operations have been proposed to improve the track ability of storms. Note that the algorithm is capable of tracking and forecasting convective cells efficiently. The performance of the algorithm is illustrated for the lifecycle of MCS. It also shows the capacity and the effectiveness of the TFCC algorithm to tackle merger and dissipation issues in the life cycle of MCS. Categorical statistics and contingency tables method applied to various case studies over China show that the proposed TFCC algorithm efficiently and accurately. Moreover, the ability of TFCC algorithm with good computational efficiency makes it a desirable choice for near-real time operational purposes, for instance, short-term forecast within 2 hours.

Acknowledgements

The authors thank the National Satellite Meteorological Center (NSMC) of China for providing satellite images. This work is supported by National Natural Science Foundation of China (Grant No. 61373063, 61373062); the project of Ministry of Industry and Information Technology of China (Grant No. E0310/1112/02-1).

References

[1] C. Morel and S. Senesi, “A climatology of mesoscale convective systems over europe using satellite infrared imagery. i: Methodology”, Quarterly Journal of the Royal Meteorological Society, vol. 128, no. 584, **(2002)**, pp. 1953–1971.

[2] C. Morel and S. Senesi, “A climatology of mesoscale convective systems over europe using satellite infrared imagery. ii: Characteristics of european mesoscale convective systems”, Quarterly Journal of the Royal Meteorological Society, vol. 128, no. 584, **(2002)**, pp. 1973–1995.

[3] R. A. Houze, “Mesoscale convective systems”, Reviews of Geophysics, vol. 42, no. 4, **(2004)**.

[4] C. Thomas, T. Corpetti and E. Mémin, "Data assimilation for convective-cell tracking on meteorological image sequences", IEEE Transactions on Geoscience and Remote Sensing, vol. 48, no. 8, **(2010)**, pp. 3162–3177.
[5] C. Thomas, T. Corpetti and E. Mémin, "Data assimilation for convective cells tracking in msg images", in IEEE International Geoscience and Remote Sensing Symposium, vol. 2, no. II–813, **(2009)**.
[6] T. Zinner, H. Mannstein and A. Tafferner, "Cb-tram: Tracking and monitoring severe convection from onset over rapid development to mature phase using multi-channel meteosat-8 seviri data", Meteorology and Atmospheric Physics, vol. 101, no. 3-4, **(2008)**, pp. 191–210.
[7] L. Machado, W. Rossow, R. Guedes and A. Walker, "Life cycle variations of mesoscale convective systems over the americas", Monthly Weather Review, vol. 126, no. 6, **(1998)**, pp. 1630–1654.
[8] B. E. Mapes and R. A. Houze Jr., "Cloud clusters and superclusters over the oceanic warm pool", Monthly Weather Review, vol. 121, no. 5, **(1993)**, pp. 1398–1416.
[9] L. Han, S. Fu, L. Zhao, Y. Zheng, H. Wang and Y. Lin, "3d convective storm identification, tracking, and forecasting-an enhanced titan algorithm", Journal of Atmospheric and Oceanic Technology, vol. 26, no.4, **(2009)**, pp. 719–732.
[10] M. Dixon and G. Wiener, "Titan: thunderstorm identification, tracking, analysis, and nowcasting-a radar based methodology", journal of atmospheric and oceanic technology, vol. 10, no. 6, **(1993)**, pp. 785–797.
[11] O. Raaf and A. El Hamid Adane, "Efficient method for detecting and tracking rainfall clouds in non-doppler radar images", Journal of Applied Remote Sensing, vol. 8, no. 1, **(2014)**.
[12] Y. Arnaud, M. Desbois and J. Maizi, "Automatic tracking and characterization of African convective systems on meteosat pictures", Journal of Applied Meteorology, vol. 31, no. 5, **(1992)**, pp. 443–453.
[13] V. Mathon and H. Laurent, "Life cycle of sahelian mesoscale convective cloud systems", Quarterly Journal of the Royal Meteorological Society, vol. 127, no. 572, **(2001)**, pp. 377–406.
[14] M. Williams and R. A. Houze Jr, "Satellite-observed characteristics of winter monsoon cloud clusters", Monthly weather review, vol. 115, no. 2, **(1987)**, pp. 505–519.
[15] D. A. Vila, L. A. T. Machado, H. Laurent and I. Velasco, "Forecast and tracking the evolution of cloud clusters (fortracc) using satellite infrared imagery: methodology and validation", Weather and Forecasting, vol. 23, no. 2, **(2008)**, pp. 233–245.
[16] B. P. Shukla and P. K. Pal, "A source apportionment approach to study the evolution of convective cells: An application to the nowcasting of convective weather systems", IEEE Journal of Selected Topics in Applied Earth Observations and Remote Sensing, vol. 5, no. 1, **(2012)**, pp. 242–247.
[17] T. Fiolleau and R. Roca, "An algorithm for the detection and tracking of tropical mesoscale convective systems using infrared images from geostationary satellite", IEEE Transactions on Geoscience and Remote Sensing, vol. 51, no. 7, **(2013)**, pp. 4302–4315.
[18] R. A. Maddox, "Mesoscale convective complexes", Bulletin of the American Meteorological Society, vol. 61, no. 11, **(1980)**, pp. 1374–1387.
[19] R. L. McAnelly and W. R. Cotton, "The precipitation life cycle of mesoscale convective complexes over the central united states", Monthly Weather Review, vol. 117, no. 4, **(1989)**, pp. 784–808.
[20] P. Soille, Morphological image analysis: principles and applications, Springer-Verlag New York, Inc., **(2003)**.
[21] J. Liu, C. Ma, C. Liu, D. Qin and X. Gu, "An extended maxima transform-based region growing algorithm for convective cell detection on satellite images", Remote Sensing Letters, vol. 5, no. 11, **(2014)**, pp. 971–980.
[22] E. L. Lawler, "Combinatorial optimization: networks and matroids", Courier Dover Publications, **(1976)**.
[23] F. Roberts and B. Tesman, "Applied combinatorics", CRC Press, **(2011)**.
[24] L. A. T. Machado and H. Laurent, "The convective system area expansion over amazonia and its relationships with convective system life duration and high-level wind divergence", Monthly Weather Review, vol. 132, no. 3, **(2004)**, pp. 714–725.
[25] J. Johnson, P. L. MacKeen, A. Witt, E. D. W. Mitchell, G. J. Stumpf, M. D. Eilts and K. W. Thomas, "The storm cell identification and tracking algorithm: An enhanced wsr-88d algorithm", Weather and Forecasting, vol. 13, no. 2, **(1998)**, pp. 263–276.
[26] V. Lakshmanan and T. Smith, "An objective method of evaluating and devising storm-tracking algorithms", Weather and Forecasting, vol. 25, no. 2, **(2010)**, pp. 701–709.
[27] V. Lakshmanan, K. Hondl and R. Rabin, "An efficient, general-purpose technique for identifying storm cells in geospatial images", Journal of Atmospheric and Oceanic Technology, vol. 26, no. 3, **(2009)**, pp. 523–537.
[28] R. M. D. Donaldson, R. J. and M. J. Kraus, "An objective evaluation of techniques for predicting severe weather events", in ninth conference on Severe Local Storms for the society of American Meteorological, **(1975)**.
[29] D. S. Wilks, "Statistical Methods in the Atmospheric Sciences", Elsevier, **(1995)**.

